

Metal Phosphonates Based on Bis(benzimidazol-2-ylmethyl)imino Methylene phosphonate: From Discrete Dimer to Two-Dimensional Network Containing Metallomacrocycles

Deng-Ke Cao, Jing Xiao, Jian-Wei Tong, Yi-Zhi Li, and Li-Min Zheng*

State Key Laboratory of Coordination Chemistry, Coordination Chemistry Institute, School of Chemistry and Chemical Engineering, Nanjing University, Nanjing 210093, P. R. China

Received June 4, 2006

Hydrothermal reactions of bis(benzimidazol-2-ylmethyl)imino(methylene phosphonic acid) $\{[(C_7H_5N_2)CH_2]_2NCH_2PO_3H_2, bbimpH_2\}$ with metal salts result in four new compounds, namely, $Mn_2\{[(C_7H_5N_2)CH_2]_2NCH_2PO_3\}_2(H_2O)_2 \cdot 2H_2O$ (**1**), $Cd_2\{[(C_7H_5N_2)CH_2]_2NCH_2PO_3\}_2 \cdot 2H_2O$ (**2**), $Fe_2\{[(C_7H_5N_2)CH_2]_2NCH_2PO_3\}_2 \cdot H_2O$ (**3**), and $Cu_2\{[(C_7H_5N_2)CH_2]_2NCH_2P(OH)O_2\}_2$ (**4**). Compounds **1** and **2** have dinuclear structures in which two $\{MN_3O_3\}$ octahedra are linked through edge sharing. In compound **3**, a chain structure is observed where the $\{FeN_3O_2\}$ trigonal bipyramids are linked by $\{CPO_3\}$ tetrahedra through corner-sharing. The structure of compound **4** is unique. The monovalent Cu(I) ions are connected by the imidazole nitrogen atoms from the $bbimp^{2-}$ ligands forming a 16-member metallomacrocyclic. These metallomacrocycles are further connected by the phosphonate oxygen atoms, leading to a two-dimensional net containing 16- and 32-member rings. Magnetic studies of **1** and **3** reveal that weak ferromagnetic interactions are mediated between magnetic centers in compound **1**, while antiferromagnetic interactions were observed in compound **3**.

Introduction

In recent years, a number of new inorganic–organic hybrid materials based on phosphonate ligands have been obtained through the incorporation of rigid or flexible organic functional groups.¹ A majority of these materials reported so far contain carboxylate or aminocarboxylate groups.² Phosphonate compounds containing N-heterocyclic groups are much fewer in number, including pyridyl³ and macrocycle groups.⁴

Bisbenzimidazole tripod ligands have been extensively studied in the syntheses of dinuclear phenoxo- or hydroxy-bridged complexes which mimic several properties of non-

heme oxo-diiron metalloenzymes.⁵ The involvement of the benzimidazole moieties in the phosphonate ligands could not only provide additional coordination sites for the metal ions but also influence the packing of the structures through weak interactions such as aromatic stacking and hydrogen-bond interactions. Thus, compounds with novel structures would be expected which may exhibit interesting properties.

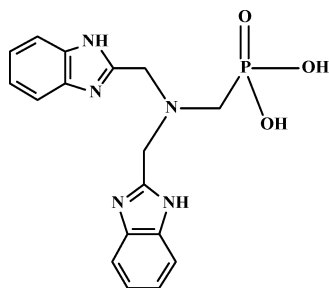
By incorporating one benzimidazol group into the diphosphonic acid, we have obtained five isostructural compounds

- (2) (a) Riou-Cavellec, M.; Sanselme, M.; Ferey, G. *J. Mater. Chem.* **2000**, *10*, 745. (b) Stock, N.; Stucky, G. D.; Cheetham, A. K. *Chem. Commun.* **2000**, 2277. (c) Fredoueil, F.; Evain, M.; Massiot, D.; Bujoli-Doeuff, M.; Janvier, P.; Clearfield, A.; Bujoli, B. *J. Chem. Soc., Dalton Trans.* **2002**, 1508. (d) Stock, N.; Frey, S. A.; Stucky, G. D.; Cheetham, A. K. *J. Chem. Soc., Dalton Trans.* **2000**, 4292. (e) Hix, G. B.; Turner, A.; Kariuki, B. M.; Tremayne, M.; MacLean, E. J. *J. Mater. Chem.* **2002**, *12*, 3220. (f) Mao, J.-G.; Wang, Z.-K.; Clearfield, A. *J. Chem. Soc., Dalton Trans.* **2002**, 4457. (g) Galdecka, E.; Galdecki, Z.; Gawryszewska, P.; Legendziewicz, J. *New J. Chem.* **2000**, *24*, 387. (h) Sagatys, D. S.; Dahlgren, C.; Smith, G.; Bott, R. C.; White, J. M. *J. Chem. Soc., Dalton Trans.* **2000**, 3404. (i) Lei, C.; Mao, J.-G.; Sun, Y.-Q.; Dong, Z.-C. *Polyhedron* **2005**, *24*, 295. (j) Mao, J.-G.; Clearfield, A. *Inorg. Chem.* **2002**, *41*, 2319. (k) Shi, X.; Zhu, G.-S.; Qiu, S.-L.; Huang, K.-L.; Yu, J.-H.; Xu, R.-R. *Angew. Chem., Int. Ed.* **2004**, *43*, 6482. (l) Vivani, R.; Costantino, U.; Nocchetti, M. *J. Mater. Chem.* **2002**, *12*, 3254. (m) Song, J.-L.; Zhao, H.-H.; Mao, J.-G.; Dunbar, K. R. *Chem. Mater.* **2004**, *16*, 1884. (n) Mao, J.-G.; Wang, Z.-K.; Clearfield, A. *New J. Chem.* **2002**, *26*, 1010.

* To whom correspondence should be addressed. E-mail: lmzheng@nju.edu.cn. Fax: +86-25-83314502.

(1) (a) Maillet, C.; Janvier, P.; Pipelier, M.; Praveen, T.; Andres, Y.; Bujoli, B. *Chem. Mater.* **2001**, *13*, 2879. (b) Hu, A.; Ngo, H. L.; Lin, W. B. *Angew. Chem., Int. Ed.* **2003**, *42*, 6000. (c) Ayyappan, P.; Evans, O. R.; Cui, Y. K.; Wheeler, A.; Lin, W. B. *Inorg. Chem.* **2002**, *41*, 4978. (d) Bauer, E. M.; Bellitto, C.; Colapietro, M.; Portalone, G.; Righini, G. *Inorg. Chem.* **2003**, *42*, 6345. (e) Kong, D.; Li, Y.; Ross, J. H.; Clearfield, A. *Chem. Commun.* **2003**, 1720. (f) Yin, P.; Gao, S.; Wang, Z.-M.; Yan, C.-H.; Zheng, L.-M.; Xin, X.-Q. *Inorg. Chem.* **2005**, *44*, 2761. (g) Nonglaton, G.; Benitez, I. O.; Guisile, I.; Pipelier, M.; Leger, J.; Dubreuil, D.; Tellier, C.; Talham, D. R.; Bujoli, B. *J. Am. Chem. Soc.* **2004**, *126*, 1497. (f) Maeda, K. *Microporous Mesoporous Mater.* **2004**, *73*, 47 and references therein.

Scheme 1



$M\{(C_7H_5N_2)CH_2N(CH_2PO_3H_2)_2\}$ ($M = Mn, Fe, Co, Cu, Cd$) showing chain structures.⁶ In this article, a new related tripodal phosphonic acid (e.g., bis(benzimidazol-2-ylmethyl)imino methylenephosphonic acid, $[(C_7H_5N_2)CH_2]_2NCH_2PO_3H_2$ (bbimpH₂), Scheme 1) is prepared. Four compounds are obtained through hydrothermal reactions of bbimpH₂ and the metal sources, including $Mn_2\{[(C_7H_5N_2)CH_2]_2NCH_2PO_3\}_2(H_2O)_2 \cdot 2H_2O$ (**1**) and $Cd_2\{[(C_7H_5N_2)CH_2]_2NCH_2PO_3\}_2 \cdot H_2O$ (**2**) with dinuclear structures, $Fe_2\{[(C_7H_5N_2)CH_2]_2NCH_2PO_3\}_2 \cdot 2H_2O$ (**3**) with a chain structure, and $Cu^{1/2}\{[(C_7H_5N_2)CH_2]_2NCH_2P(OH)_2\}_2$ (**4**) with a unique layer structure.

Experimental Section

Bis(acetic acid)imino methylenephosphonic acid was prepared according to the literature method.⁷ All other reagents were purchased as reagent grade chemicals and used without further purification. Elemental analyses were performed on a Perkin-Elmer 240C elemental analyzer. The IR spectra were obtained as KBr disks on a VECTOR 22 spectrometer. Variable-temperature magnetic susceptibility data were obtained on microcrystalline samples (5.08 mg for **1**, 14.91 mg for **3**) from 1.8 to 300 K in a magnetic field of 2 kOe, using a Quantum Design MPMS-XL7 SQUID magnetometer. Diamagnetic corrections were made for both the sample holder and the compound, estimated from Pascal's constants.⁸

Synthesis of Bis(benzimidazol-2-ylmethyl)imino Methylenephosphonic Acid (bbimpH₂). The synthetic procedure is similar to that for the preparation of bibmpH₄.⁶ Bis(acetic acid)imino methylenephosphonic acid (25 mmol, 5.7 g) and 1,2-diaminobenzene (50 mmol, 5.41 g) were fully mixed by grinding. The mixture was transferred into an open single-neck flask and heated at 190 °C until no steam released. After the resulting green solid was cooled, hydrochloric acid (6 M, 10 mL) was added. The solution was refluxed at 120 °C for 3 h and then left at room temperature overnight. Green crystals were filtered and recrystallized in hot distilled water and then in hot methanol. Light green needlelike crystals were collected, washed with ethanol, and dried in air. Yield: 5.65 g (53%). Anal. Found (calcd) for $C_{17}H_{18}N_5O_3P \cdot 3H_2O$: C, 48.46 (48.00); H, 5.64 (5.65); N, 16.50 (16.47)%. IR (KBr, cm^{-1}): 3444(m), 3379(m), 3155–2507(br), 1856(w), 1624(m), 1575(w), 1522(w), 1496(w), 1459(m), 1439(w), 1420(w), 1399(w), 1346(w), 1298(w), 1245(m), 1220(m), 1140(m), 1126(m), 1104(s), 1066(s), 1014(m), 978(m), 928(m), 905(m), 891(m), 826(w), 762(m), 746(m), 704(w), 669(w), 618(m), 579(w), 546(w), 504(w), 473(m), 448(w). The thermal analysis revealed a weight loss of 11.6% between 24 and 270 °C, close to the calculated value (12.7%) for the release of three water molecules.

Synthesis of $Mn_2\{[(C_7H_5N_2)CH_2]_2NCH_2PO_3\}_2(H_2O)_2 \cdot 2H_2O$ (1**).** A mixture of bbimpH₂·3H₂O (0.10 mmol, 0.0425 g), $MnCl_2 \cdot 4H_2O$ (0.10 mmol, 0.0198 g), and 0.072 g of 25% Me₄NOH in 8 mL of H₂O (pH 7.4) was kept in a Teflon-lined autoclave at 140 °C for 24 h. After the mixture was cooled to room temperature, light yellow blocky crystals were obtained, together with a small amount of unidentified brown powder. The crystals were manually selected and were used for physical measurements. Yield: 28 mg (61% based on bbimpH₂). Anal. Found (calcd) for $C_34H_{40}N_{10}O_{10}P_2 \cdot Mn_2$: C, 44.31 (44.32); H, 4.31 (4.34); N, 15.23 (15.21)%. IR (KBr, cm^{-1}): 3424(s), 2974(w), 2928(w), 1655(w), 1648(w), 1638(w), 1626(w), 1536(w), 1509(w), 1489(w), 1468(m), 1456(s), 1399(w), 1333(w), 1316(w), 1290(w), 1226(w), 1130(s), 1108s, 1052s, 1035(s), 1003(w), 983(w), 959(m), 946(w), 916(w), 766(w), 750(m), 596(w), 574(w), 498(w), 487(w), 435(w). Thermal analysis revealed a weight loss of 8.0% over the temperature range of 98–143 °C resulting from the removal of two lattice and two coordination water molecules (calcd 7.8%). Then a plateau is observed up to 305 °C, above which the compound is completely decomposed.

Synthesis of $Cd_2\{[(C_7H_5N_2)CH_2]_2NCH_2PO_3\}_2 \cdot H_2O$ (2**).** A mixture of bbimpH₂·3H₂O (0.1 mmol, 0.0425 g) and $CdSO_4 \cdot 2.7H_2O$ (0.1 mmol, 0.0253 g) in 8 mL of H₂O, adjusted to pH 3.5–4.6 with 1 M NaOH, was kept in a Teflon-lined autoclave at 140 °C for 24 h. After the mixture was cooled to room temperature, colorless blocky crystals were collected as a monophasic material, based on the powder XRD measurement. Yield: 30 mg (62% based on bbimpH₂). Anal. Found (calcd) for $C_{34}H_{34}N_{10}O_7P_2Cd_2$: C, 41.55 (41.57); H, 3.39 (3.46); N, 14.29 (14.26)%. IR (KBr, cm^{-1}): 3415(m), 3265–2654(br), 1657(w), 1648(w), 1623(w), 1593(w), 1600(w), 1542(w), 1533(w), 1486(w), 1472(m), 1453(s), 1436(m), 1398(w), 1342(w), 1314(w), 1279(m), 1230(m), 1128(m), 1115(m), 1092(s), 1055(s), 1032(s), 1003(w), 988(w), 968(w), 949(s), 915(w), 896(w), 871(w), 845(w), 766(m), 758(m), 735(s), 704(w), 668(w), 643(w), 629(w), 589(w), 572(m), 547(m), 527(w), 498(w), 477(w), 440(w), 414(w). Thermal analysis showed that the removal of one lattice water molecule (calcd 1.8%) occurred between 120 and 356 °C with a weight loss of 1.9%. Above 356 °C, the organic ligand decomposed, and the structure collapsed.

Synthesis of $Fe_2\{[(C_7H_5N_2)CH_2]_2NCH_2PO_3\}_2 \cdot 2H_2O$ (3**).** A mixture of bbimpH₂·3H₂O (0.10 mmol, 0.0425 g), $FeSO_4 \cdot 7H_2O$ (0.10 mmol, 0.0278 g), and 0.074 g of 25% Me₄NOH in 8 mL of

- (3) (a) Ayyappan, P.; Evans, O. R.; Foxman, B. M.; Wheeler, K. A.; Warren, T. H.; Lin, W. B. *Inorg. Chem.* **2001**, *40*, 5954. (b) Yi, X.-Y.; Zheng, L.-M.; Xu, W.; Feng, S. H. *J. Chem. Soc., Dalton Trans.* **2003**, 953. (c) Gan, X.-M.; Binyamin, I.; Rapko, B. M.; Fox, J.; Duesler, E. N.; Paine, R. T. *Inorg. Chem.* **2004**, *43*, 2443. (d) Vermeulen, L. A.; Fateen, R. Z.; Robinson, P. D. *Inorg. Chem.* **2002**, *41*, 2310. (e) Song, J. L.; Mao, J.-G.; Sun, Y. Q.; Clearfield, A. *Eur. J. Inorg. Chem.* **2003**, 4218. (f) Cao, D.-K.; Liu, Y.-J.; Song, Y.; Zheng, L.-M. *New J. Chem.* **2005**, *29*, 721. (g) Cao, D.-K.; Li, Y.-Z.; Zheng, L.-M. *Inorg. Chem.* **2005**, *44*, 2984. (h) Cao, D.-K.; Li, Y.-Z.; Song, Y.; Zheng, L.-M. *Inorg. Chem.* **2005**, *44*, 3599.
- (4) (a) Bligh, S. W. A.; Choi, N.; Geraldes, C. F. G. C.; Knoke, S.; McPartlin, M.; Sangane, M. J.; Woodroffe, T. M. *J. Chem. Soc., Dalton Trans.* **1997**, 4119. (b) Sharma, C. V. K.; Clearfield, A. *J. Am. Chem. Soc.* **2000**, *122*, 1558. (c) Kotek, J.; Lubal, P.; Hermann, P.; Cisarova, I.; Lukes, I.; Godula, T.; Svobodova, I.; Taborsky, P.; Havel, J. *Chem.—Eur. J.* **2003**, *9*, 233. (d) Hassfjell, S.; Kongshaug, K. O.; Romming, C. *Dalton Trans.* **2003**, 1433. (e) Kong, D. Y.; Medvedev, D.G.; Clearfield, A. *Inorg. Chem.* **2004**, *43*, 7308. (f) Guerra, K. P.; Delgado, R.; Lima, L. M. P.; Drew, M. G. B.; Felix, V. *Dalton Trans.* **2004**, 1812. (g) Kong, D.; Clearfield, A. *Chem. Commun.* **2005**, 1005. (h) Mao, J.-G.; Wang, Z.-K.; Clearfield, A. *Inorg. Chem.* **2002**, *41*, 3713. (i) Bao S.-S.; Chen G.-S.; Wang Y.; Li, Y.-Z.; Zheng L.-M.; Luo Q.-H. *Inorg. Chem.* **2006**, *45*, 1124.
- (5) (a) Satcher, J. H., Jr.; Droege, M. W.; Olmstead, M. M.; Balch, A. L. *Inorg. Chem.* **2001**, *40*, 1454. (b) Gomez-Romero, P.; Casan-Pastor, N.; Ben-Hussein, A.; Jameson, G. B. *J. Am. Chem. Soc.* **1988**, *110*, 1988. (c) Rapta, M.; Kamaras, P.; Brewer, G. A.; Jameson, G. B. *J. Am. Chem. Soc.* **1995**, *117*, 12865.
- (6) Cao, D.-K.; Xiao, J.; Li, Y.-Z.; Clemente-Juan, J. M.; Coronado, E.; Zheng, L.-M. *Eur. J. Inorg. Chem.* **2006**, 1830.
- (7) Moedritzer, K.; Irani, R. R. *J. Org. Chem.* **1966**, *31*, 1603.
- (8) Kahn, O. *Molecular Magnetism*; VCH Publishers: New York, 1993.

Table 1. Crystallographic Data and Refinement Parameters for Compounds 1–4

	1	2	3	4
empirical formula	C ₃₄ H ₄₀ N ₁₀ O ₁₀ P ₂ Mn ₂	C ₃₄ H ₃₄ N ₁₀ O ₇ P ₂ Cd ₂	C ₃₄ H ₃₄ N ₁₀ O ₇ P ₂ Fe ₂	C ₃₄ H ₃₄ N ₁₀ O ₆ P ₂ Cu ₂
fw	920.58	981.45	868.35	867.73
cryst syst	monoclinic	monoclinic	triclinic	monoclinic,
space group	<i>P</i> 2 ₁ / <i>c</i>	<i>C</i> 2/ <i>c</i>	<i>P</i> $\bar{1}$	<i>P</i> 2 ₁ / <i>c</i>
<i>a</i> (Å)	12.962(2)	20.617(4)	9.5807(14)	11.4778(14)
<i>b</i> (Å)	10.0892(17)	13.973(4)	9.9959(15)	13.1159(15)
<i>c</i> (Å)	16.049(2)	14.040(3)	11.4230(17)	24.903(3)
α (deg)			84.330(3)	
β (deg)	116.516(11)	120.515(5)	85.224(3)	102.761(3)
γ (deg)			62.268(3)	
<i>V</i> (Å ³)	1878.1(5)	3484.5(13)	962.7(2)	3656.3(8)
<i>Z</i>	2	4	1	4
ρ_{calcd} (g cm ⁻³)	1.628	1.871	1.498	1.576
<i>F</i> (000)	948	1960	446	1776
<i>R</i> _{int}	0.0343	0.0406	0.0323	0.0501
GOF on <i>F</i> ²	1.122	0.982	1.079	1.018
R1, wR2 [<i>I</i> > 2 σ (<i>I</i>)] ^a	0.0515, 0.1032	0.0381, 0.0906	0.0617, 0.1394	0.0587, 0.1094
R1, wR2 (all data) ^a	0.0709, 0.1078	0.0509, 0.0952	0.0727, 0.1428	0.1107, 0.1197
($\Delta\rho$) _{max} , ($\Delta\rho$) _{min} (e Å ⁻³)	0.258, -0.455	0.769, -0.643	0.400, -0.477	0.439, -0.569

$$^a R1 = \sum |F_o| - |F_c| / \sum |F_o|, wR2 = [\sum w(F_o^2 - F_c^2)^2 / \sum w(F_o^2)]^{1/2}.$$

H₂O (pH 5.2) was kept in a Teflon-lined autoclave at 140 °C for 24 h. After the mixture was cooled to room temperature, yellow needlelike crystals were obtained together with a small amount of unidentified brown powder. The crystals were manually selected and were used for physical measurements. Yield: 11 mg (25%). Anal. Found (calcd.) for C₃₄H₃₆N₁₀O₈P₂Fe₂: C, 45.98 (46.03); H, 4.21 (4.06); N, 15.65 (15.80)%. IR (KBr, cm⁻¹): 3385(m), 3099–2642(br), 1625(w), 1598(w), 1545(w), 1487(w), 1470(s), 1454(s), 1438(m), 1402(w), 1344(m), 1318(w), 1281(m), 1248(w), 1225(w), 1131(s), 1087(s), 1064(s), 1032(s), 996(s), 963(m), 914(m), 888(w), 845(w), 753(s), 736(s), 666(w), 654(w), 633(w), 593(m), 556(w), 514(w), 501(w), 436(w), 407(w). Thermal analysis showed a weight loss of 4.1% in the temperature range of 51–174 °C, in agreement with the release of two lattice water molecules (calcd 4.1%).

Synthesis of Cu^I₂[(C₇H₅N₂)CH₂]₂NCH₂P(OH)O₂]₂ (4). A mixture of bbimpH₂·3H₂O (0.10 mmol, 0.0638 g) and CuSO₄ (0.10 mmol, 0.0160 g) in 10 mL of H₂O, adjusted to pH 5.05 with 1 M NaOH, was kept in a Teflon-lined autoclave at 140 °C for 24 h. After the mixture was cooled to room temperature, light yellow needlelike crystals were obtained together with a small amount of unidentified brown powder. The crystals were manually selected and were used for physical measurements. Yield: 12 mg (28%). Anal. Found (calcd.) for C₃₄H₃₄N₁₀O₆P₂Cu₂: C, 47.28 (47.02); H, 4.05 (3.92); N, 16.18 (16.13)%. IR (KBr, cm⁻¹): 3426(m), 3173–2781(br), 1626(w), 1598(w), 1542(w), 1488(w), 1458(s), 1429(m), 1396(w), 1367(w), 1346(w), 1317(w), 1280(m), 1257(w), 1224(m), 1210(m), 1157(s), 1128(m), 1095(w), 1056(s), 1039(s), 1001(w), 968(w), 920(s), 910(s), 883(w), 861(w), 762(w), 740(s), 671(w), 650(w), 631(w), 576(w), 560(m), 543(s), 500(w), 476(m), 459(w), 427(w), 416(w).

X-ray Crystallographic Studies. Single crystals of dimensions 0.10 × 0.04 × 0.04 mm for **1**, 0.15 × 0.10 × 0.10 mm for **2**, 0.08 × 0.05 × 0.05 mm for **3**, and 0.10 × 0.05 × 0.05 mm for **4** were used for structural determination on a Bruker SMART APEX CCD diffractometer using graphite-monochromated Mo K α radiation (λ = 0.71073 Å) at room temperature. A hemisphere of data was collected in the θ range of 2.47–26.00° for **1**, 2.40–25.99° for **2**, 1.79–25.00° for **3**, and 1.85–26.00° for **4**, using a narrow-frame method with scan widths of 0.30° in ω and an exposure time of 5 s/frame. Numbers of measured and observed reflections [*I* > 2 σ (*I*)] are 9527 and 3662 (*R*_{int} = 0.0343) for **1**, 8992 and 3410 (*R*_{int} = 0.0406) for **2**, 4760 and 3980 (*R*_{int} = 0.0323) for **3**, and 19 465

Table 2. Selected Bond Lengths (Å) and Angles (deg) for Compound 1^a

Mn1–O1	2.200(2)	Mn1–N1	2.575(3)
Mn1–O1W	2.271(2)	Mn1–N2	2.154(3)
Mn1–O1A	2.097(2)	Mn1–N4	2.169(3)
P1–O1	1.545(2)	P1–O2	1.511(2)
P1–O3	1.504(2)		
N2–Mn1–O1	93.0(1)	O1A–Mn1–O1	77.3(1)
N4–Mn1–O1	101.9(1)	O1A–Mn1–N1	152.9(1)
N2–Mn1–N4	134.3(1)	N2–Mn1–N1	72.2(1)
N2–Mn1–O1W	88.0(1)	N4–Mn1–N1	70.1(1)
N4–Mn1–O1W	88.7(1)	O1–Mn1–N1	75.9(1)
O1–Mn1–O1W	164.0(1)	O1W–Mn1–N1	119.4(1)
O1A–Mn1–O1W	87.6(1)	O1A–Mn1–N2	113.2(1)
O1A–Mn1–N4	112.2(1)	Mn1A–O1–Mn1	102.8(1)
P1–O1–Mn1	125.4(1)	C10–N2–Mn1	131.5(2)
P1–O1–Mn1A	131.8(1)	C4–N2–Mn1	120.4(2)
C1–N1–Mn1	104.8(2)	C11–N4–Mn1	118.9(2)
C2–N1–Mn1	109.1(2)	C17–N4–Mn1	134.3(2)
C3–N1–Mn1	104.5(2)		

^a Symmetry transformations used to generate equivalent atoms: (A) $-x + 1, -y + 1, -z + 2$.

and 7180 (*R*_{int} = 0.0501) for **4**, respectively. The data were integrated using the Siemens SAINT program,⁹ with the intensities corrected for Lorentz factor, polarization, air absorption, and absorption due to variation in the path length through the detector faceplate. Multiscan absorption corrections were applied. The structures were solved by direct methods and were refined on *F*² by full-matrix least squares using SHELXTL.¹⁰ All the non-hydrogen atoms were located from the Fourier maps and were refined anisotropically. All H atoms were refined isotropically, with the isotropic vibration parameters related to the non-H atom to which they are bonded. Crystallographic and refinement details of **1–4** are listed in Table 1. Selected bond lengths and angles are given in Tables 2–5.

Results and Discussion

Syntheses. Compounds **1–4** were obtained through hydrothermal reactions of bbimpH₂ and the corresponding metal

(9) SAINT, Program for Data Extraction and Reduction; Siemens Analytical X-ray Instruments: Madison, WI, 1994–1996.

(10) SHELXTL, version 5.0; Siemens Industrial Automation, Analytical Instruments: Madison, WI, 1997.

Table 3. Selected Bond Lengths (Å) and Angles (deg) for Compound 2^a

Cd1—O1	2.355(3)	Cd1—N1	2.502(3)
Cd1—O2A	2.191(3)	Cd1—N2	2.244(4)
Cd1—O1A	2.679(3)	Cd1—N4	2.306(3)
P1—O1	1.539(3)	P1—O3	1.511(3)
P1—O2	1.515(3)		
O1—Cd1—N1	72.3(1)	O2A—Cd1—N4	111.8(1)
N2—Cd1—O1	95.5(1)	O2A—Cd1—O1	102.4(1)
N4—Cd1—O1	126.3(1)	O2A—Cd1—N2	108.9(1)
N4—Cd1—N1	72.4(1)	O2A—Cd1—N1	174.6(1)
N2—Cd1—N4	110.1(1)	C1—N1—Cd1	104.5(2)
N2—Cd1—N1	71.9(1)	C2—N1—Cd1	107.6(2)
N4—Cd1—N1	72.4(1)	C3—N1—Cd1	106.7(2)
O2A—Cd1—O1	102.4(1)	C4—N2—Cd1	116.3(3)
Cd1—O1—Cd1A	104.9(1)	C10—N2—Cd1	137.1(3)
P1—O1—Cd1	118.5(2)	C11—N4—Cd1	114.2(3)
P1—O2—Cd1A	105.1(1)	C17—N4—Cd1	137.9(3)
P1—O1—Cd1A	84.96(12)	O1—Cd1—O1A	75.1(1)

^a Symmetry transformations used to generate equivalent atoms: (A) $-x + 1/2, -y + 1/2, -z + 2$.

Table 4. Selected Bond Lengths (Å) and Angles (deg) for Compound 3^a

Fe1—O1	1.980(6)	Fe2—O2	1.936(6)
Fe1—O4A	1.931(7)	Fe2—O6	1.962(6)
Fe1—N2	2.165(8)	Fe2—N7	2.098(8)
Fe1—N4	2.098(7)	Fe2—N9	2.131(7)
Fe1—N1	2.502(7)	Fe2—N6	2.455(7)
P1—O1	1.520(7)	P2—O4	1.519(7)
P1—O2	1.520(6)	P2—O5	1.501(6)
P1—O3	1.501(7)	P2—O6	1.521(7)
O1—Fe1—N4	121.5(3)	O6—Fe2—O2	101.9(3)
O1—Fe1—N2	117.8(3)	O2—Fe2—N7	98.1(3)
N4—Fe1—N2	103.0(3)	O2—Fe2—N9	112.1(3)
O4A—Fe1—O1	102.4(3)	O6—Fe2—N7	120.8(3)
O4A—Fe1—N4	104.6(3)	O6—Fe2—N9	115.1(3)
O4A—Fe1—N2	106.0(3)	N7—Fe2—N9	107.3(3)
O4A—Fe1—N1	175.6(3)	O2—Fe2—N6	173.1(3)
O1—Fe1—N1	80.6(3)	O6—Fe2—N6	81.7(3)
N4—Fe1—N1	71.0(3)	N7—Fe2—N6	75.0(3)
N2—Fe1—N1	75.2(3)	N9—Fe2—N6	70.9(3)
C3—N1—Fe1	105.8(5)	C21—N7—Fe2	117.7(7)
C2—N1—Fe1	104.9(5)	C27—N7—Fe2	136.1(6)
C1—N1—Fe1	104.2(5)	C28—N9—Fe2	114.8(6)
C4—N2—Fe1	114.1(7)	C34—N9—Fe2	133.6(5)
C10—N2—Fe1	132.6(5)	C20—N6—Fe2	107.9(5)
C11—N4—Fe1	119.4(6)	C19—N6—Fe2	103.6(5)
C17—N4—Fe1	135.5(5)	C18—N6—Fe2	101.9(5)
P1—O1—Fe1	127.2(4)	P2—O4—Fe1B	167.8(4)
P1—O2—Fe2	158.2(4)	P2—O6—Fe2	125.7(4)

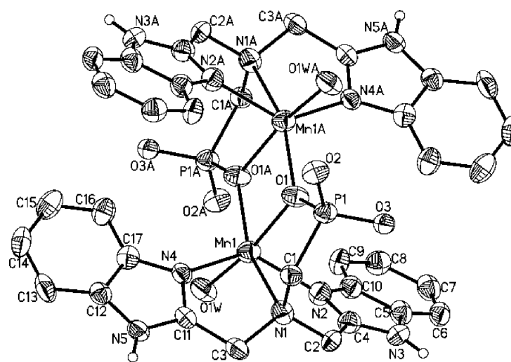
^a Symmetry transformations used to generate equivalent atoms: (A) $x + 1, y, z$; (B) $x - 1, y, z$.

ions at 140 °C for 1 day. To investigate factors that may affect the formation of the final products, a series of experiments have been conducted by changing the molar ratio of the starting materials, the metal sources, the pH values, and the base to adjust the pH of the reaction mixture. It is found that pure phases of compound **2** with good yields can be obtained when the molar ratio of M/ligand and the pH are 1:1 and 3.5–4.6, respectively. For compounds **1**, **3**, and **4**, crystallization of the products is always accompanied by the formation of brown powder impurities when the molar ratio of M/ligand and the pH are 1:0.57–1.70 and 2.92–7.49 for **1**, 1:0.43–1.70 and 2.56–5.66 for **3**, and 1:0.43–1.70 and 2.37–7.00 for **4**, respectively. Samples with the best crystal quality and relatively high yields were obtained when M/ligand = 1:0.8, pH 7.4 for **1**, M/ligand = 1:0.83,

Table 5. Selected Bond Lengths (Å) and Angles (deg) for Compound 4^a

Cu(1)—N(2)	1.889(4)	Cu(2)—N(4)	1.908(3)
Cu(1)—N(9)	1.949(3)	Cu(2)—N(7)	1.906(4)
Cu(1)—O(1A)	2.100(3)	Cu(2)—O(4B)	2.093(3)
P(1)—O(1)	1.528(3)	P(2)—O(4)	1.527(3)
P(1)—O(2)	1.512(3)	P(2)—O(5)	1.512(3)
P(1)—O(3)	1.605(4)	P(2)—O(6)	1.565(3)
N(2)—Cu(1)—N(9)	150.8(2)	C(28)—N(9)—Cu(1)	128.5(3)
N(2)—Cu(1)—O(1A)	109.9(1)	C(34)—N(9)—Cu(1)	123.9(3)
N(9)—Cu(1)—O(1A)	99.2(1)	C(11)—N(4)—Cu(2)	129.1(3)
N(4)—Cu(2)—N(7)	150.4(2)	C(17)—N(4)—Cu(2)	124.0(3)
N(4)—Cu(2)—O(4B)	100.3(1)	C(20)—N(7)—Cu(2)	130.5(3)
N(7)—Cu(2)—O(4B)	108.7(1)	C(26)—N(7)—Cu(2)	122.6(3)
C(9)—N(2)—Cu(1)	122.4(3)	P(1)—O(1)—Cu(1C)	148.1(2)
C(3)—N(2)—Cu(1)	131.4(3)	P(2)—O(4)—Cu(2D)	146.6(2)

^a Symmetry transformations used to generate equivalent atoms: (A) $-x + 1, y - 1/2, -z + 1/2$; (B) $-x + 2, y + 1/2, -z + 1/2$; (C) $-x + 1, y + 1/2, -z + 1/2$; (D) $-x + 2, y - 1/2, -z + 1/2$.

**Figure 1.** Dinuclear structure of compound **1**. Thermal ellipsoids are at the 50% probability level. All H atoms except H3B and H5A are omitted for clarity.

pH 5.2 for **3**, and M/ligand = 1:1, pH 5.05 for **4**. In the preparation of compounds **1**, **3**, and **4**, different metal sources such as metal sulfate, metal acetate, and metal halide were tried, and $\text{MnCl}_2 \cdot 4\text{H}_2\text{O}$, $\text{FeSO}_4 \cdot 7\text{H}_2\text{O}$, and CuSO_4 were found to be the best in getting products with high crystal quality. It is also noted that either Me_4NOH or NaOH can be used to adjust the pH of the reaction mixtures in the synthesis of compounds **2** and **4**, whereas Me_4NOH is essential in the preparation of crystalline materials of **1** and **3**. When we replace CuSO_4 by CuCl , the same compound **4** was obtained, together with some unidentified brown powder. Finally, a longer reaction time (>24 h) would result in more brown powders.

Crystal Structure of 1. Compound **1** crystallizes in monoclinic space group $P2_1/c$. It has a centrosymmetrically related dinuclear structure (Figure 1). The asymmetric unit contains one Mn(II) ion, one bbimp^{2-} ligand, one coordinated water molecule, and one lattice water molecule. The Mn atom is six-coordinated with a distorted octahedral environment. Four of the six bonding sites are occupied by the phosphonate oxygen (O1) and three nitrogen atoms (N1, N2, and N4) from the same bbimp^{2-} ligand. The remaining sites are filled with the phosphonate oxygen atom (O1A) from the other equivalent bbimp^{2-} ligand and the water molecule (O1W). The Mn1—N bond lengths (2.154(3)–2.575(3) Å) are in agreement with those in compounds $[\text{Mn}(\text{NTB})-(\text{C}_8\text{H}_4\text{O}_4) \cdot \text{DMF} \cdot 0.5\text{CH}_3\text{OH} \cdot 0.5\text{H}_2\text{O}]$ (2.136(5)–2.526(4) Å)

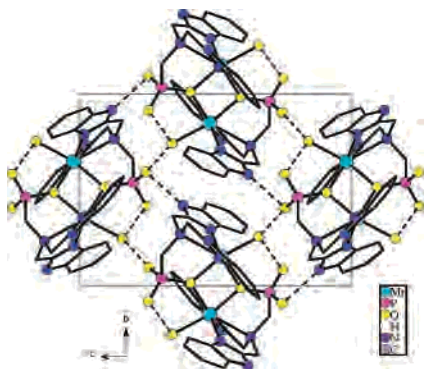


Figure 2. One layer of structure 1 viewed along the *a* axis.

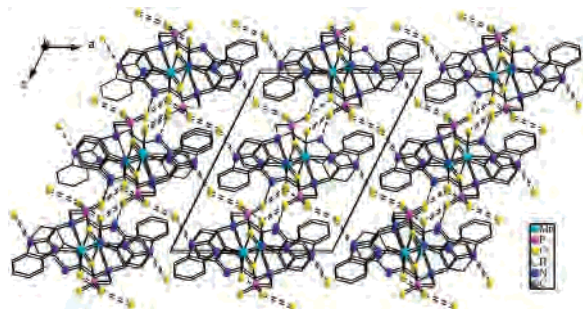


Figure 3. Packing diagram of structure 1 projected along the *b* axis.

(NTB = tris(2-benzimidazolyl-methyl)amine)¹¹ and $[\text{LMn}_2(\text{CH}_3\text{CO}_2)(\text{butanol})(\text{ClO}_4)\cdot 2\text{H}_2\text{O}]$ (2.129(8)–2.475(7) Å) (*L* = *N,N,N',N'*-tetrakis(2-methylenebenzimidazole)-1,3-diaminopropan-2-ol),¹² although the *Mn1*–*N1* distance in 1 (2.575(3) Å) is significantly longer. The *Mn1*–*O* lengths are in the range of 2.097(2)–2.271(2) Å.

Each bbimp^{2-} ligand serves as a tetradentate ligand and chelates the Mn atom through one amino nitrogen (*N1*), two imidazole nitrogens (*N2*, *N4*), and one phosphonate oxygen (*O1*). The phosphonate oxygen (*O1*) acts as a μ_3 -O and bridges the two equivalent Mn atoms into a dimer. The *Mn1*–*O1*–*Mn1A* bond angle is 102.8(1)°, and the *Mn*···*Mn* distance is 3.358 Å. The remaining two phosphonate oxygen atoms (*O2*, *O3*) are pendent and are involved in the hydrogen-bonding network, together with the benzimidazol nitrogen atoms (*N3*, *N5*) and water molecules (*O1W*), forming a supramolecular layer in the *bc* plane (Figure 2). The *O(N)*···*O* distances are 2.744(3) Å for *O(1W)*···*O(2ⁱ)*, 2.754(3) Å for *O(1W)*···*O(3ⁱⁱ)*, and 2.767(3) Å for *N(3)*···*O(3^{iv})*. These layers are packed along the *a* axis with the lattice water molecules residing between the layers (Figure 3). The *O(2W)*···*O(N)* distances are 2.908(4) Å for *N(5)*···*O(2Wⁱⁱⁱ)* and 2.703(3) Å for *O(2W)*···*O(2^{iv})* (symmetry codes: (i) $-x + 1, -y + 1, -z + 2$; (ii) $x, -y + 3/2, z + 1/2$; (iii) $x - 1, y, z$; (iv) $-x + 1, y + 1/2, -z + 3/2$).

Crystal Structure of 2. Compound 2 crystallizes in the monoclinic space group *C2/c*. It has a dimeric structure closely related to that of compound 1 (Figure 4). The Cd(II) ion also adopts a distorted octahedral geometry with four

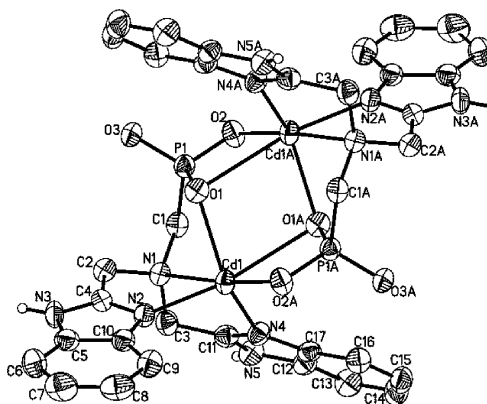


Figure 4. Dinuclear structure of compound 2. Thermal ellipsoids are at the 50% probability level. All H atoms except H3B and H5A are omitted for clarity.

positions occupied by three N atoms and one O atom from the same bbimp^{2-} ligand (*N1*, *N2*, *N4*, and *O1*). The remaining two positions are filled with two phosphonate oxygen atoms (*O1A* and *O2A*) from the other equivalent bbimp^{2-} ligand. The Cd–N bond lengths fall in the range of 2.244(4)–2.502(3) Å, in agreement with those in $[\text{Cd}(\text{NTB})\text{NO}_3]\text{NO}_3\cdot 3\text{H}_2\text{O}$ (2.228(3)–2.690(3) Å).¹³ The $\{\text{CdN}_3\text{O}_3\}$ octahedra are edge-shared through phosphonate oxygen atom *O1*, forming a dimer. The *Cd1*–*O1*–*Cd1A* bond angle is 104.9(1)°, which is slightly larger than that in 1. The Cd···Cd distance across the oxygen bridge (3.996 Å) is also longer than the *Mn*···*Mn* distance (3.358 Å) in 1.

The bbimp^{2-} ligand in compound 2 behaves as a pentadentate ligand by using one imino nitrogen (*N1*), two imidazole nitrogens (*N2*, *N4*), and two phosphonate oxygens (*O1*, *O2*). The *O1* atom acts as a μ_3 -O bridge and links the two equivalent Cd atoms into a dimer, hence forming a four-member ring with a small *O1*–*Cd1*–*O1A* angle (75.1(8)°). The bond length of *Cd1*–*O1A* (2.679(3) Å) is significantly longer than the other Cd–O distances (2.191(3) and 2.355(3) Å).

Extensive hydrogen-bond interactions are found between the dimers among the phosphonate oxygen atoms (*O1*, *O3*), the protonated imidazole nitrogen atoms (*N3*, *N5*), and the lattice water molecules (*O1w*). The *O1w*···*O3ⁱ*, *N3*···*O1ⁱⁱ*, and *N5*···*O3ⁱⁱⁱ* distances are 2.904(4), 2.814(5), and 2.812(4) Å, respectively (symmetry codes: (i) $-x + 1, y + 1, -z + 3/2$; (ii) $-x + 1, y, -z + 5/2$; (iii) $x, -y, z - 1/2$). The π – π stacking is found between the benzimidazol rings along *c* axis, considering that the centroid–centroid distance between the two phenyl rings of the benzimidazol groups is 3.854 Å for 2 (Figure 5).¹⁴ A three-dimensional supramolecular structure is therefore constructed.

Crystal Structure of 3. Compound 3 crystallizes in triclinic space group *P1̄*. The asymmetric unit contains two crystallographically independent Fe(II) ions, two bbimp^{2-} ligands, and two lattice water molecules. Both Fe atoms adopt distorted trigonal bipyramidal geometries (Figure 6). The

(11) Xiang, D.-F.; Tan, X.-S.; Hang, Q.-W.; Tang, W.-X.; Wu, B.-M.; Mak, T. C. W. *Inorg. Chim. Acta* 1998, 277, 21.

(12) Pessiki, P. J.; Khangulov, S. V.; Ho, D. M.; Dismukes, G. C. *J. Am. Chem. Soc.* 1994, 116, 891.

(13) Quiroz-Castro, E.; Bernes, S.; Barba-Behrens, N.; Tapia-Benavides, R.; Contreras, R.; Noth, H. *Polyhedron* 2000, 19, 1479

(14) Janiak, C. *J. Chem. Soc., Dalton Trans.* 2000, 3885.

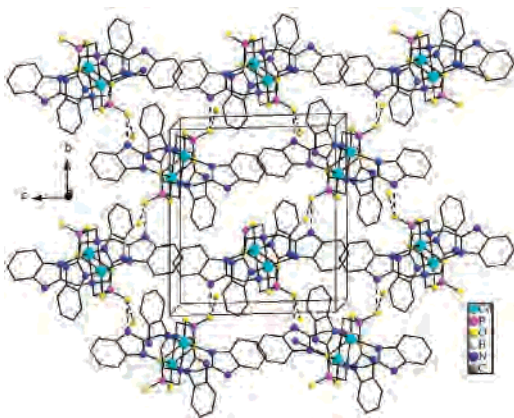


Figure 5. Packing diagram of structure 2 viewed down the *a* axis.

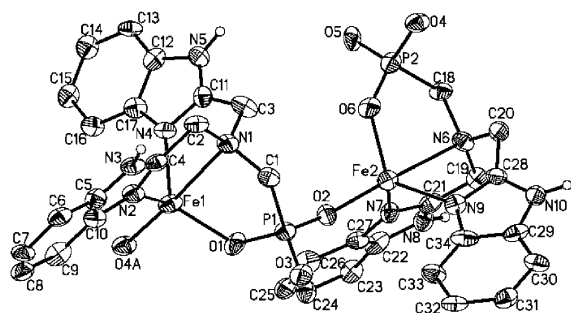


Figure 6. Building unit of structure 3. Thermal ellipsoids are at the 50% probability level. All H atoms except H3B, H5B, H8A, and H10A are omitted for clarity.

basal sites are provided by two benzimidazol nitrogens and one phosphonate oxygen from the same ligand (O1, N2, and N4 for Fe1 and O6, N7, and N9 for Fe2). The Fe atoms deviate from the basal planes by 0.507 Å for Fe1 and 0.493 Å for Fe2, respectively. The axial positions are occupied by one imino nitrogen and one phosphonate oxygen atoms from two bbimp²⁻ ligands (N1 and O4A for Fe1 and N6 and O2 for Fe2). The axial Fe–N distances (2.502(7) Å for Fe1–N1 and 2.455(7) Å for Fe2–N6) are much longer than the other Fe–N distances (2.098(7)–2.165(8) Å). They are also longer than a similar bond in Fe₂(BMDP)(OBz)(SCN)₂ (2.327(18) Å).¹⁵ The Fe–O bond lengths are in the range of 1.931(7)–1.980(6) Å.

Each bbimp²⁻ ligand in **3** acts as a pentadentate ligand. It chelates to the same Fe atom using one phosphonate oxygen, one imino nitrogen, and two benzimidazol nitrogens (O1, N1, N2, and N4 for Fe1 and O6, N6, N7, and N9 for Fe2). One of the two remaining phosphonate oxygen atoms of each {CPO₃} terminus (O2, O4) coordinates to the neighboring Fe atoms. Accordingly, a chain is formed along the *a* axis through corner-sharing of {FeN₃O₂} trigonal bipyramids and {CPO₃} tetrahedra (Figure 7). The Fe···Fe distances across the O–P–O bridges are 5.769 Å for Fe1···Fe2 and 5.717 Å for Fe2···Fe1A, respectively.

Between the chains, there are extensive hydrogen-bonding interactions among the imidazole nitrogen, phosphonate oxygen, and water molecules. The N3···O5ⁱ, N8···O3ⁱⁱ, and

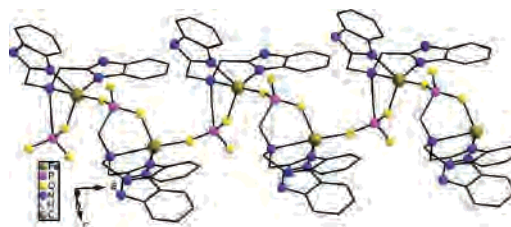


Figure 7. Fragment of the chain in structure 3. All H atoms are omitted for clarity.

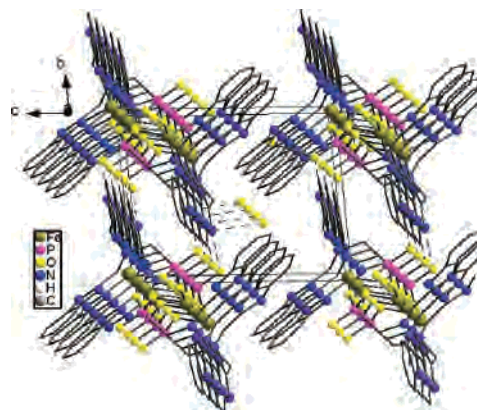


Figure 8. Packing diagram of structure 3 projected along the *a* axis.

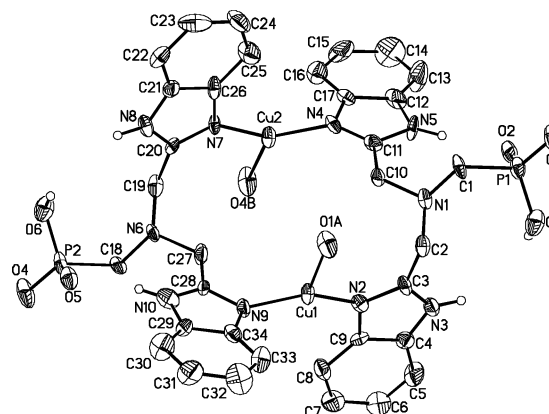


Figure 9. Building unit of structure 4. Thermal ellipsoids are at the 50% probability level. All H atoms except H3B, H5B, H8A, H10A, H3A, and H6C are omitted for clarity.

N5...O1wⁱⁱⁱ distances are 2.715(10), 2.696(11), and 3.053-(19) Å, respectively (symmetry codes: (i) *x*, *y* + 1, *z*; (ii) *x*, *y* – 1, *z*; (iii) *x*, *y*, *z* – 1). The π – π interactions are also found between the benzimidazol rings from adjacent chains along the *c* axis. The centroid–centroid distance between the two phenyl rings of the benzimidazol groups is 3.516 Å (Figure 8).

Crystal Structure of 4. Compound **4** crystallizes in monoclinic space group *P*₂₁/*c*. The asymmetric unit of the structure consists of two independent Cu atoms and two bbimpH⁻ ligands. Both Cu atoms are monovalent and three-coordinated, with the three sites provided by two imidazole nitrogens and one phosphonate oxygen (Figure 9). The Cu–N bond lengths are in the range of 1.889(4)–1.949(3) Å, comparable to those in [Cu₂(*μ*-I)₂(2-PhBim)₂]₂·2THF (1.969(5) Å)¹⁶ and [Cu^I(L₁-Pr)][BF₄] (L₁-Pr = 2,2'-bis(2-(*N*-propylbenzimidazolyl))diethyl sulfide) (1.910(5)–1.912-

(15) Satcher, J. H., Jr.; Balch, A. L.; Olmstead, M. M.; Droegge, M. W. *Inorg. Chem.* **1996**, *35*, 1749

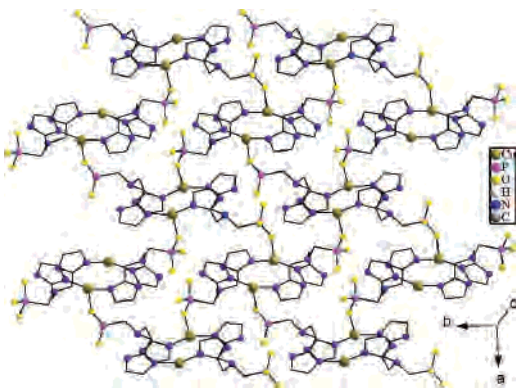


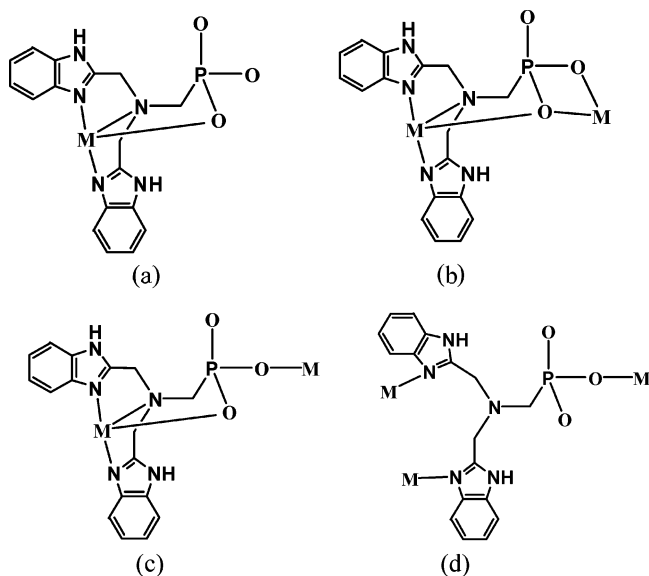
Figure 10. One net-shaped layer of structure **4**. All H atoms and phenyl rings of the benzimidazol groups are omitted for clarity.

(5) Å).¹⁷ The N–Cu–N bond angles are 150.8(2)–150.4(2)°. The Cu–O distances are 2.100(3)–2.093(3) Å, slightly shorter than that in $\text{Cu}_2\text{Cu}^{\text{II}}(\text{hedpH}_2)_2(4,4'\text{-bipy})_2\cdot 2\text{H}_2\text{O}$ (2.237(3) Å).¹⁸

The bbimpH[−] ligands are each tridentate, using two imidazole nitrogens (N2, N4 and N7, N9) and one phosphonate oxygen (O1 and O4). The two bbimpH[−] ligands are bridged by two Cu(I) ions through the coordination of imidazole nitrogen atoms, forming a metallomacrocyclic, a 16-membered ring (Figure 9). The two CH₂PO₃ groups behave like two arms which stretch out from two opposite sides of the ring. Each arm links a Cu atom from a neighboring macrocycle ring, resulting in a unique two-dimensional network containing 16- and 32-member rings (Figure 10). One of the remaining two phosphonate oxygen atoms of each CPO₃ terminus is protonated (P1–O3 = 1.605–(4) Å and P2–O6 = 1.565(3) Å). Hydrogen bonds are found among the phosphonate oxygen atoms (O2, O3, O5, and O6) and the benzimidazol nitrogen atoms (N3, N5, N8, and N10). Three shortest contacts are 2.587(4) Å for O3⋯O5ⁱ, and 2.824(5) Å for N5⋯O2 and N8⋯O2ⁱⁱ (symmetry codes: (i) $x, y + 1, z$; (ii) $x, y - 1, z$) (Figure 11).

Comparison of the Structures. As is well-known, bis-benzimidazole tripodal ligands can be used in the syntheses of dinuclear phenoxo-bridged or hydroxy-bridged complexes. The bis(benzimidazol-2-ylmethyl)imino methylenephosphonate (bbimp^{2−}), which incorporates a methylenephosphonate group, shows similar coordination capabilities. Thus, dinuclear compounds **1** and **2** are also obtained. In both structures, one imino nitrogen and two imidazole nitrogen atoms are involved in the coordination with metal ions. One phosphonate oxygen atom serves as a μ_3 -O bridge and links the two equivalent metal atoms into a dimer. Compared with compound **1**, however, two phosphonate oxygen atoms coordinate to the same Cd atom in compound **2** (Scheme 2a and b), hence forming a four-member ring with a small O–Cd–O angle. The basic unit of structure **3** is very similar to those of **1** and **2**. In the latter case, however, two of the three phosphonate oxygen atoms are each coordinated to a

Scheme 2



single Fe atom, leading to the formation of a chain structure (Scheme 2c). The structure of compound **4** is ubiquitous. In this case, the Cu(II) ions in the reaction mixture are reduced to Cu(I) which are linked by imidazole nitrogen atoms of bbimp^{2−}, forming a 16-member metallomacrocyclic. These metallomacrocycles are further bridged by the phosphonate oxygen atoms, forming an interesting layer structure containing 16- and 32-member rings. The imino nitrogen atom is not involved in the coordination with Cu(I) ions (Scheme 2d). To the best of our knowledge, similar layer structures have not been observed previously in the metal phosphonate compounds.

Magnetic Properties. Figure 12 shows the $\chi_{\text{M}}T$ and χ_{M}^{-1} versus T plots for compound **1**. The room-temperature effective magnetic moment (μ_{eff}) is 6.16 μ_{B} per Mn, close to the expected spin-only value (5.92 μ_{B}) for isolated spin $S = 5/2$ with $g = 2$. In the whole temperature range, the magnetic behavior follows the Curie–Weiss law with a Curie constant of 9.16 $\text{cm}^3 \text{K mol}^{-1}$ and a Weiss constant of +1.38 K. The positive Weiss constant indicates a ferromagnetic interaction between the magnetic centers. When it is cooled from room temperature, the $\chi_{\text{M}}T$ value increases with

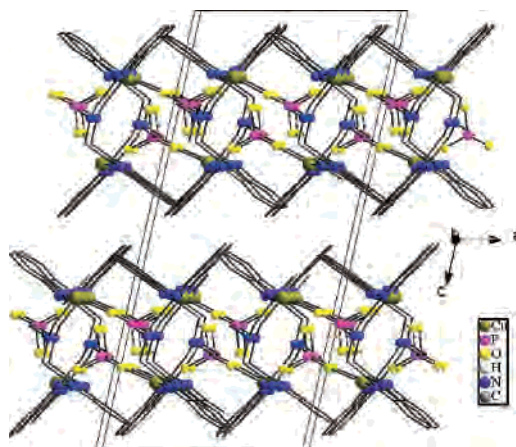


Figure 11. Packing diagram of **4** projected along the b axis.

(16) Toth, A.; Floriani, C.; Chiesi-Villa, A.; Guastinil, C. *Inorg. Chem.* **1987**, *26*, 3897.

(17) Dagdigian, J. V.; Mckee, V.; Reed, C. A. *Inorg. Chem.* **1982**, *21*, 1332.

(18) Zheng, L.-M.; Yin, P.; Xin, X.-Q. *Inorg. Chem.* **2002**, *41*, 4084.

$$\chi'_M = \frac{2Ng^2\beta^2}{kT} \frac{\exp(2J/kT) + 5 \exp(6J/kT) + 14 \exp(12J/kT) + 30 \exp(20J/kT) + 55 \exp(30J/kT)}{1 + 3 \exp(2J/kT) + 5 \exp(6J/kT) + 7 \exp(12J/kT) + 9 \exp(20J/kT) + 11 \exp(30J/kT)}$$

$$\chi_M = \frac{\chi'_M}{1 - (zj'/Ng^2\beta^2)\chi'_M}$$

decreasing temperature, confirming a ferromagnetic exchange between the Mn(II) ions. Since compound **1** has a dinuclear structure in which the Mn(II) ions are doubly bridged by phosphonate oxygen atoms, the magnetic susceptibility data can be analyzed by the following expression based on a Heisenberg Hamiltonian $H = -2JS_1S_2$,⁸ where $2J$ is the coupling constant, N , g , β , and k have their usual meanings, and zj' accounts for the interdimer exchange. The best fit, shown as the solid line in Figure 12, results in parameters $g = 2.03$, $2J = 0.72 \text{ cm}^{-1}$, and $zj' = -0.0085 \text{ cm}^{-1}$. The magnetization measured at 2 K is $4.99 N_\beta$ at 70 kOe, close to the value of $5.0 N_\beta$ anticipated for a spin $S = 5/2$ with $g = 2.0$ (Supporting Information). Weak ferromagnetic interactions were also found in a few μ -O bridged Mn(II) compounds such as $[\text{Mn}_2\text{LX}]$ (L = macrocyclic ligands, X = Cl^- or Br^- , $2J = 0.22\text{--}0.60 \text{ cm}^{-1}$)¹⁹ and $[\text{Mn}(\text{hfac})_2(4\text{-cpyNO})_2]$ ($2J = 0.23 \text{ cm}^{-1}$).²⁰

Compound **3** has a chain structure in which the Fe(II) ions are bridged by O–P–O units. Usually the Fe(II) ion in an octahedral environment shows a significant single-ion anisotropy or spin-orbital coupling. When the symmetry of the molecule is lowered, however, the orbital contribution could be partially removed. In the case of compound **3**, each Fe atom has a strongly distorted trigonal bipyramidal geometry. The orbital contributions of Fe(II) would be largely reduced. Indeed, the μ_{eff} per Fe(II) at 300 K ($5.04 \mu_B$) is very close to

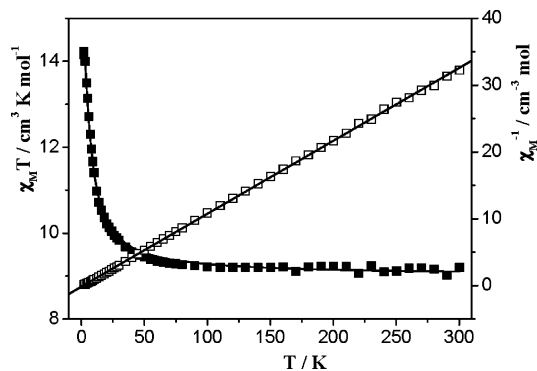


Figure 12. $\chi_M T$ and χ_M^{-1} vs T plots for **1**.

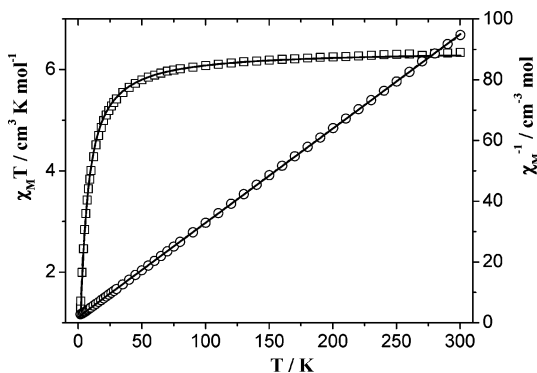


Figure 13. $\chi_M T$ and χ_M^{-1} vs T plots for **3**.

the spin-only value of $4.90 \mu_B$ for an isolated spin $S = 2$ with $g = 2$.

Figure 13 shows the $\chi_M T$ and χ_M^{-1} versus T plots for compound **3**. Clearly, the magnetic behavior in the temperature range of 1.8–300 K follows the Curie–Weiss law with a Weiss constant of -6.08 K and a Curie constant of $3.22 \text{ cm}^3 \text{ K mol}^{-1}$. The continuous decreasing of $\chi_M T$ upon cooling suggests a dominant antiferromagnetic interaction between the Fe(II) ions. The susceptibility data were initially fitted by Fisher's formula with $S = 2$ but failed. When we look at the structure carefully, the Fe \cdots Fe distances across the O–P–O bridges are 5.769 \AA for Fe1 \cdots Fe2 and 5.717 \AA for Fe2 \cdots Fe1A. Therefore, the chain structure of compound **3** may be viewed as being composed of {Fe1–O–P1–O–Fe2} dimers connected by O–P2–O units. The magnetic data were thus analyzed by a modified Fisher's expression based on the Heisenberg Hamiltonian, $\mathbf{H} = -\sum J_{\text{Ai}} \mathbf{S}_{\text{Ai}} \mathbf{S}_{\text{Ai}+1}$,²¹

$$\chi_d = \frac{2Ng^2\beta^2}{kT} S_d(S_d + 1)$$

$$\chi_d = \frac{2Ng^2\beta^2}{kT} \frac{6e^{2J_d/kT} + 30e^{6J_d/kT} + 84e^{12J_d/kT} + 180e^{20J_d/kT}}{1 + 3e^{2J_d/kT} + 5e^{6J_d/kT} + 7e^{12J_d/kT} + 9e^{20J_d/kT}}$$

$$\chi_M = \frac{Ng^2\beta^2}{3kT} \frac{1 + u}{1 - u} S_d(S_d + 1)$$

$$u = \coth(J_c S_d(S_d + 1)/kT) - kT/J_c S_d(S_d + 1)$$

where J_c and J_d are the inter- and intradimer coupling constants, respectively. This expression reduces to the classical uniform chain when the S value of the metal ion takes the place of S_d . A good fit, shown as the solid line in Figure 13, gives parameters $g = 2.06$, $J_c = -0.131 \text{ cm}^{-1}$, and $J_d = -0.310 \text{ cm}^{-1}$. The small J value is consistent with the other O–P–O bridged compounds such as Fe- $\{(\text{C}_7\text{H}_5\text{N}_2)\text{CH}_2\text{N}(\text{CH}_2\text{PO}_3\text{H})_2\}$ (-0.33 cm^{-1}).⁶

Conclusions. By using bis(benzimidazol-2-ylmethyl)imino methylenephosphonic acid $\{[(\text{C}_7\text{H}_5\text{N}_2)\text{CH}_2]_2\text{NCH}_2\text{PO}_3\text{H}_2, \text{bbimpH}_2\}$, we obtained four new compounds under hydrothermal conditions. Compounds $\text{Mn}_2\{[(\text{C}_7\text{H}_5\text{N}_2)\text{CH}_2]_2\text{NCH}_2\text{PO}_3\}_2 \cdot (\text{H}_2\text{O})_2 \cdot 2\text{H}_2\text{O}$ (**1**) and $\text{Cd}_2\{[(\text{C}_7\text{H}_5\text{N}_2)\text{CH}_2]_2\text{NCH}_2\text{PO}_3\}_2 \cdot \text{H}_2\text{O}$ (**2**) have similar dinuclear structures in which two $\{\text{MN}_3\text{O}_3\}$ octahedra are linked through edge sharing. In compound $\text{Fe}_2\{[(\text{C}_7\text{H}_5\text{N}_2)\text{CH}_2]_2\text{NCH}_2\text{PO}_3\}_2 \cdot 2\text{H}_2\text{O}$ (**3**), a chain structure is observed where the $\{\text{FeN}_3\text{O}_2\}$ trigonal

(19) Luneau, D.; Savariault, J. M.; Cassoux, P.; Tuchagues, J. P. *J. Chem. Soc., Dalton Trans.* **1988**, 1225.

(20) Ryazanov, M.; Troyanov, S.; Baran, M.; Szymczak, R.; Kuzmina, N. *Polyhedron* **2004**, *23*, 879.

(21) Kou, H.-Z.; Zhou, B.-C.; Liao, D.-Z.; Wang, R.-J.; Li, Y. *Inorg. Chem.* **2002**, *41*, 6887.

bipyramids are linked by $\{\text{CPO}_3\}$ tetrahedra through corner-sharing. The structure of compound $\text{Cu}^{\text{I}}_2\{[(\text{C}_7\text{H}_5\text{N}_2)\text{CH}_2]_2\text{-NCH}_2\text{P}(\text{OH})\text{O}_2\}_2$ (**4**) is unexpected; it contains 16-member metallomacrocycles connected by the phosphonate oxygen atoms into a layer. Magnetic studies of **1** and **3** reveal that weak ferromagnetic interactions are mediated between magnetic centers in compound **1**, while antiferromagnetic interactions were observed in compound **3**.

Acknowledgment. The authors thank the NNSF of China (No. 20325103) and the specialized research fund for the

doctoral program of the Ministry of Education of China (No. 0205116201) for financial support, Mr. Yong-Jiang Liu for crystal data collection, and Dr. Y. Song for magnetic measurements.

Supporting Information Available: X-ray crystallographic files in CIF format for the four compounds, TG curves for compounds **1–3**, and field-dependent magnetization for compound **1**. This material is available free of charge via the Internet at <http://pubs.acs.org>. IC060990A